



Research on the Establishment of Secondary Monitoring Indicators for the Lock Head of High Slope-Reinforced Navigation Locks

Yachao Wang^{1,a}, Haoran Wang^{2,b}, Yantao Zhu^{3,*}

¹Changjiang Survey, Planning, Design and Research Co., Ltd., Wuhan 430010, China

²College of Water Conservancy and Hydropower Engineering, Hohai University, Nanjing, 210024, China

³College of Water Conservancy and Hydropower Engineering, Hohai University, Nanjing, 210024 and National Dam Safety Research Center, Wuhan, 430010, China

Email: ^awangyachao@cjwsjy.com.cn, ^bwang_haoran@hhu.edu.cn

*Corresponding author, Email: zhuyantao@hhu.edu.cn

Abstract. The establishment of scientifically sound deformation monitoring indicators is essential for ensuring the safety and serviceability of navigational structures. This study examines a large, reinforced lock-head structure and proposes secondary deformation monitoring indicators by employing a hybrid approach that combines structural analysis and statistical modeling of deformations. First, a structural analysis method is used to assess the rock foundation by strength reduction, analyzing both the plastic zone's evolution and the trends in displacement at various monitoring points. This strength-reduction approach generates a water-level component that is then combined with a time-dependent component of the deformation, a temperature component, and the reference deformation at both side slopes. Ultimately, secondary deformation monitoring indicators are established for the lock head and side slopes, offering practical reference value for engineering applications.

Keywords: High Slope-Reinforced Navigation Locks; Lock Head; Secondary Monitoring Indicators; combined force

1 Introduction

Deformation monitoring is a fundamental safety measure that provides a direct and reliable reflection of the structural deformation and stress state. With sufficient monitoring data gathered during operational phases, deformation indicators are frequently used to evaluate a structure's resilience under potential load conditions[1]. These indicators serve as permissible bounds for the magnitude and rate of deformation under various load combinations, reflecting the structure's service state[2]. Establishing scientifically grounded deformation monitoring indicators enables accurate assessment of structural safety, which is crucial for ensuring the safety and functional integrity of navigational structures[3].

© The Author(s) 2025

Y. Qiu et al. (eds.), *Proceedings of the 2024 7th International Conference on Civil Architecture, Hydropower and Engineering Management (CAHEM 2024)*, Advances in Engineering Research 256, https://doi.org/10.2991/978-94-6463-650-5_48

Concrete structures typically exhibit three phases in their mechanical response: linear elasticity, elasto-plasticity, and stability loss. According to standards for the safety monitoring of concrete dams, structural behavior is categorized into normal, abnormal, and critical stages, with corresponding monitoring indicators classified into primary, secondary, and tertiary levels. Significant research has been conducted to define these safety monitoring indicators, with methods introduced by various scholars. For instance, Cong et al.[4] utilized a maximum entropy approach to determine dam safety indicators and tested their reliability using the A-D method. Li et al.[5] integrated motion stability theory and finite element analysis to set deformation indicators, discussing the advantages and limitations of commonly used threshold-setting methods.

In current research, two main approaches are widely applied. The first method relies on monitoring data sequences, utilizing techniques such as confidence interval analysis, low-probability statistical methods, and cloud modeling. The second approach employs a hybrid model combining structural analysis and statistical modeling of deformations[6]. The first method, while straightforward, lacks clear physical definitions and fails to incorporate actual material parameters, limiting its explanatory power. The hybrid approach, in contrast, leverages both structural and bedrock mechanics, effectively integrating empirical data with design parameters. It can simulate unfavorable conditions beyond what the statistical model alone can predict, making it broadly applicable and improving the accuracy of deformation monitoring indicators[3].

Navigational locks are critical components of hydraulic structures, with the lock head being particularly vital for water retention, stress distribution, deformation, and stability control. Despite substantial progress in defining safety monitoring indicators for dams, research focused specifically on locks, particularly high-slope reinforced lock-head structures, remains limited. The reinforced lock chamber structure is often used in mountainous rivers, leveraging the combined load-bearing capacity of both bedrock and the lock walls to handle vessel loads, water pressure, and other forces. Its structural safety has strong representativeness and is a key part of the stability control of the high slope of the ship lock[7]. This configuration enhances both economic efficiency and applicability. Unlike conventional lock-head monitoring indicator methods, monitoring reinforced lock-head structures requires consideration of the interaction between the lock head and the side slopes. Statistical methods are not suitable for large-scale, high-priority projects due to poor interpretability. Typical low-probability approach is also inapplicable when deformation convergence is not achieved. Numerical methods demand require extensive parameters, such as properties for temperature and aging calculations. Thus, finding interpretable, low-complexity monitoring indicators for high-slope lined ship locks is valuable in theory and practice[8]. Therefore, this study examines the lock head of a large reinforced lock structure, analyzing sensitivity to gate opening and the deterioration of rock mass mechanical parameters. It also considers the stability of the lock-head structure, the plastic zone development trends, and annual temperature variations. Using a hybrid modeling approach, this study establishes secondary monitoring indicators for horizontal deformation in the lock head.

2 Principles for Establishing Secondary Deformation Monitoring Indicators for Reinforced Lock-Head Structures

A deterministic model requires calculating the effect field of the dam and foundation under various loads using the finite element method. By iteratively fitting these results to empirical data and adjusting parameters, a model is established, though it is labor-intensive. In defining secondary deformation indicators for concrete structures under unfavorable loading conditions, the structure generally remains in a viscoelastic state, requiring elastoplastic parameters to compute the water pressure and temperature components, while viscoelastic-plastic parameters are used for time-dependent effects. However, numerous elastic, strength, and viscosity parameters for the lock-head and bedrock are difficult to obtain accurately, making it challenging to establish reliable deformation monitoring indicators. The hybrid model helps address limitations in both statistical and deterministic models.

Given the relative reliability and modest size of parameters for calculating the water pressure component, a hybrid model based on numerical computation and statistical analysis was used to establish deformation indicators for the lock head. This model integrates the combined load-bearing properties of the reinforced lock head and side slopes, accounting for deformation across both to determine the final monitoring indicators.

In practice, the hybrid model is first applied to calculate the deformation indicators for measurement points on the side slopes and the corresponding strength reduction factor. The model then calculates the water-level component and strength reduction factor for the lock head under different water level conditions, which are compared with those of the side slopes, taking the lower of the two. Lastly, the water-level component is combined with time-dependent and temperature components obtained via statistical modeling to establish secondary deformation monitoring indicators for the lock head, expressed as:

$$[\delta] = \delta_H + \delta_T + \delta_\theta \quad (1)$$

Where $[\delta]$ represents the secondary deformation monitoring indicator, δ_H is the water pressure component under unfavorable conditions, δ_T is the temperature component during peak seasonal variation, and δ_θ is the time-dependent component.

3 Application Case

3.1 Project Overview

The project consists of a dual-line, multi-stage lock system, with the two lock lines arranged in parallel and deeply excavated into natural mountainous terrain, creating high rock slopes on both sides. The slope height varies from 100 to 160 meters. The lock head, classified as a primary structure, is a 70-meter long, 59-meter high reinforced structure. The bedrock, primarily fresh granite, contains no weathered layers or weak

foundation. Weathered and weak rock layers in the areas between the lock piers and on both slopes have been excavated and backfilled with soil. Horizontal displacement of the lock structure is monitored using inverted plumb lines. Considering the characteristics of structural deformation and measurement point layout, horizontal displacements at two top measurement points PL03CZ331 on the north line and PL05CZ321 on the right pier of the south line are used as indicators for the lock-head structure. For slope monitoring, the highest deformation points on both slope tops TPBM10GP01 and TPBM28GP02 were selected.

3.2 Finite Element Model Parameters and Grid Division

In finite element analysis, the Drucker-Prager criterion is applied to the bedrock and slope rock formations, while a concrete plastic damage model is used for the concrete structure. The model includes the three lock heads and both side slopes, with boundary ranges extending 60 meters below the lock chamber floor and outward three times the lock chamber width on each bank. The model comprises 660,723 elements and 679,698 nodes, as illustrated in Figure 1. Rock and concrete material parameters for the lock head and side slopes were derived through structural inversion analysis.

Long-term concrete testing (90 days to 10 years) has shown increased compressive and tensile strength over time. Given the high quality of construction, degradation of concrete mechanical parameters is considered negligible. However, external factors such as blasting, unloading, water impoundment, and seepage erosion can degrade rock mechanics parameters. Thus, strength reduction scenarios for rock materials are calculated.

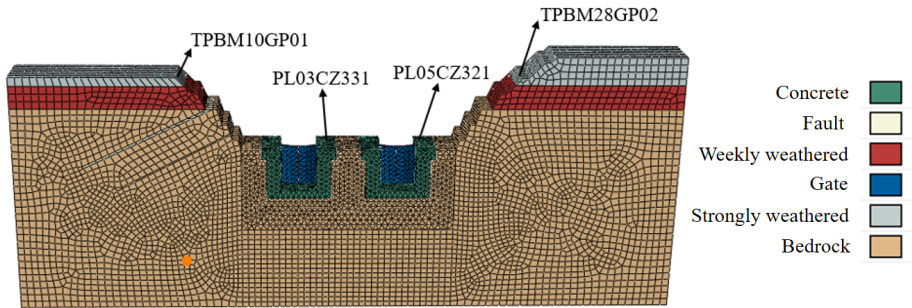


Fig. 1. Model and Grid Division of the Lock Head and Side Slopes

3.3 Establishing Secondary Deformation Indicators for Side Slopes

Methodology. The excavation of the lock head and side slopes was completed over 20 years ago, with slope deformation stabilizing since then. Monitoring data indicates that slope deformation primarily results from rock unloading, with minimal impact from temperature or rainfall.

To establish secondary deformation monitoring indicators, monitoring data from the cutoff date was used as a reference. The model first balanced ground stress on the lock head and side slopes to nullify pre-existing stress effects on slope deformation, then applied water and uplift pressures on the lock chamber and foundation. Sensitivity analysis was conducted on strength parameters to determine deformation after strength reduction. The secondary monitoring indicator combines deformation from strength reduction and pre-stress equilibrium deformation.

Since reverse dip faulting within the side slopes minimally impacts overall slope stability, strength reduction is simultaneously applied to both bedrock and fault parameters. The maximum deformation point, located on the higher south slope, is analyzed independently, as slope deformation monitoring must factor in water level variations inside the lock chamber.

Secondary Deformation Monitoring Indicators for the South Slope. Strength reduction analysis was performed on the lock head and both side slopes, yielding deformation trends for the south slope as the reduction factor increased, as shown in Figure 2. Results indicate that slope deformation increased with higher reduction factors. When the reduction factor reached 6.8, a plastic zone appeared at the contact between the rock and lock head concrete. Displacement at the measurement point towards the free face increased significantly, indicating the slope was entering an accelerated instability phase. The displacement at the slope top measurement point at this time reflects the deformation induced by parameter reduction. By adding this displacement change to the displacement recorded at the reference point (cut-off date of the monitoring data), the secondary deformation monitoring indicator for the south slope top measurement point TPBM28GP02 is established, as shown in Table 1.

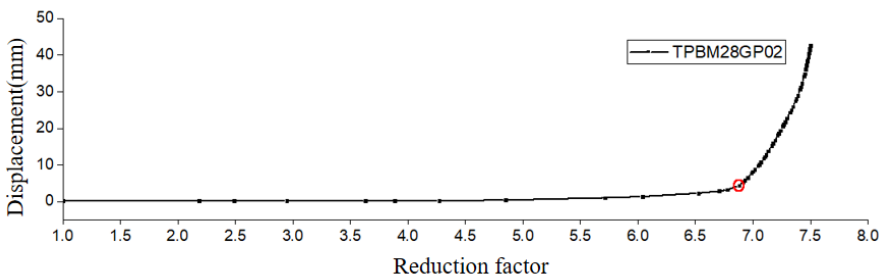


Fig. 2. Displacement trend of TPBM28GP02 under varying reduction factors

Table 1. Secondary Deformation Monitoring Indicator for TPBM28GP02 (mm)

Measurement Point ID	Displacement during Reduction	Reference Displacement	Monitoring Indicator	Measured Maximum	Difference with Max
TPBM28GP02	5.42	46.89	52.31	46.89	5.42

Secondary Deformation Monitoring Indicators for the North Slope. Strength reduction analysis was conducted on the lock head and north slope, with the range and results shown in Figures 3 and 4. As seen, slope deformation increased as the reduction factor rose. When the reduction factor reached 8.1, a plastic zone emerged at the rock-lock head concrete interface. Displacement towards the free face at the measurement point increased sharply, signifying that the slope had entered an accelerated instability state. Following the same method, the secondary deformation monitoring indicator for the north slope measurement point TPBM10GP01 was determined, as shown in Table 2.

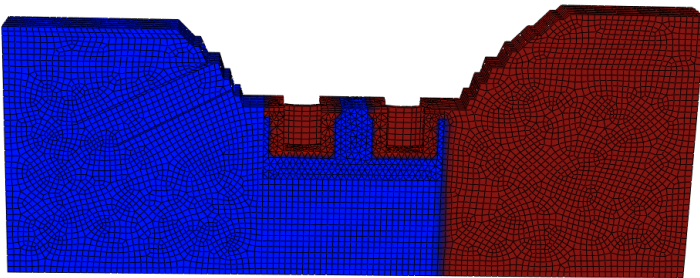


Fig. 3. Strength reduction range on the north slope (blue indicates reduction area)

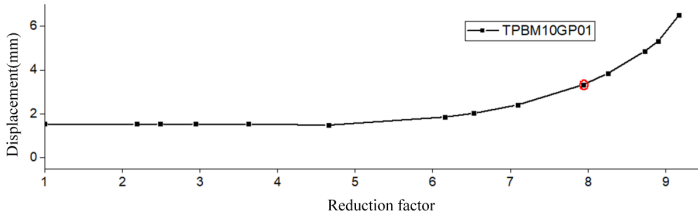


Fig. 4. Displacement trend of TPBM10GP01 towards under varying reduction factors

Table 2. Secondary Deformation Monitoring Indicator for TPBM10GP01 (mm)

Measurement Point ID	Displacement during Reduction	Reference Displacement	Monitoring Indicator	Measured Maximum	Difference with Max
TPBM10GP01	3.85	54.25	58.1	54.25	3.85

3.4 Secondary Deformation Monitoring Indicators for the Lock Head

The deformation of the lock head piers is composed of water pressure, temperature, and time-dependent components. Therefore, in setting secondary deformation monitoring indicators, the water pressure component determined by parameter reduction is combined with temperature and time-dependent components derived from monitoring data

through statistical modeling. The final deformation monitoring indicator results from the integration of these three components. Trial calculations showed that deformation at the lock pier measurement points towards the lock chamber is heavily influenced by south slope deformation, necessitating simultaneous strength reduction calculations on both the rock and structural surface for the lock head deformation monitoring indicator.

Due to the variance in inward deformation of the lock piers under different water levels, the lock head secondary deformation monitoring indicator is divided into two categories: one for normal operating conditions and another for low water levels. The indicator for normal operating conditions applies across various water level conditions, with the water level set at 141.1 m upstream and 118.5 m downstream. For low water conditions, the indicator corresponds to flood prevention water levels, with upstream and downstream water levels set at 134.62 m and 113.88 m, respectively.

Effect of Gate Opening on Lock Head Deformation. Different gate opening levels affect lock-head deformation. The study calculated lock-head deformation at normal water levels with gate openings at 0°, 30°, and 60°, as shown in Table 3. Deformation was minimal when the gate was closed, so indicators are based on the closed-gate condition to ensure broad applicability.

Table 3. Displacement towards the Chamber Side under Different Gate Opening Angles (mm)

Measurement Point	Gate Closed	Gate Opening at 30°	Gate Opening at 60°
PL01CZ121	1.14	2.01	1.45
PL01CZ131	0.96	1.07	0.97

Calculation of Water Level Components with Material Reduction Factors. Figure 5 shows deformation trends for PL05CZ321 and PL03CZ331 at normal water levels as the reduction factor increases. When the reduction factor reached 6.0, displacement in the direction of the lock chamber increased sharply, defining the water pressure component for the monitoring indicator under normal conditions. Similarly, a reduction factor of 5.9 was used under low water level conditions, as shown in Figure 6 and Table 4.

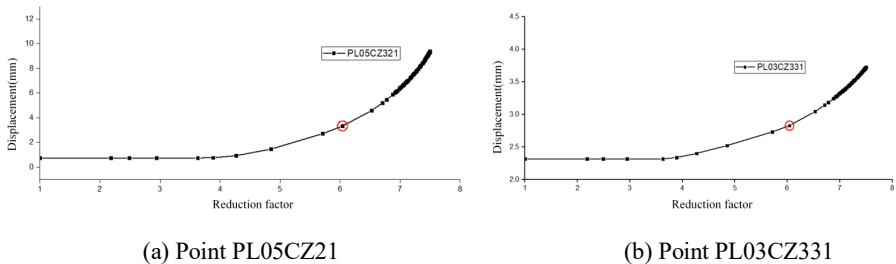


Fig. 5. Variation of Displacement for PL05CZ21 and PL03CZ331 under Normal Conditions with Different Reduction Factors

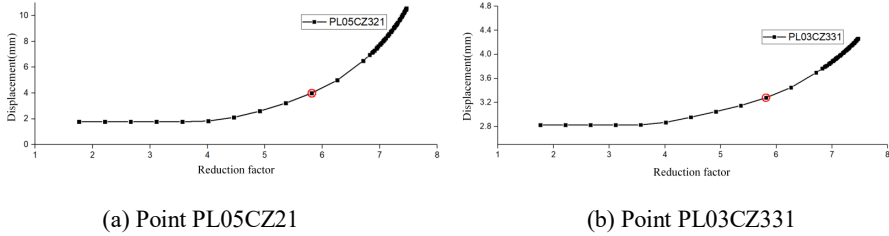


Fig. 6. Variation of Displacement for PL05CZ21 and PL03CZ331 under Low Water Level Conditions with Different Reduction Factors

Table 4. Water Component for Measurement Points under Operational Conditions (mm)

Operational Condition	Measurement Point ID	Water Level Component
Normal Operation	PL03CZ331	2.82
	PL05CZ321	3.31
Low Water Condition	PL03CZ331	3.28
	PL05CZ321	3.99

Calculation of Temperature and Time-Dependent Components via Statistical Modeling. In accordance with safety monitoring theory, when higher levels of safety monitoring are required, a temperature component is established using an HTT-based statistical model[9]. While more complex than HST, this model offers improved fitting accuracy, represented by the following formula:

$$\delta = \delta_H + \sum_{i=0}^6 b_i T_i + e_1 \ln(1 + t) + e_2 t \tag{2}$$

Where δ_H is the water-level component obtained from structural analysis in section 3.4.2, and $T_0 \sim T_6$ represent average and peak temperatures recorded on the observation date and at various intervals: the past 7, 15, 30, 60, 90, and 120 days, respectively. Additionally, t represents the number of days since the initial measurement date, December 15, 2001.

Given the significant annual temperature variation in the reservoir area, using only the annual maximum temperature for the secondary indicator would yield considerable error. Thus, this study adopts a model that applies maximum monthly temperatures over several years to determine the temperature component. As the structure deteriorates, temperature effects also increase. Therefore, this study adds half of the annual amplitude to the temperature component as a correction for deformation. The time-dependent and adjusted temperature components derived from the statistical model are summarized in Table 5.

Table 5. Temperature and Time-Dependent Components for Lock Head Measurement Points

Measurement Point	Temperature Component (mm)				Time-Dependent
	Dec.-Feb.	Mar.-May	Jun.-Aug.	Sept.-Nov.	

					Component (mm)
PL03CZ331	0.79	0.96	1.62	1.38	2.86
PL05CZ321	1.59	1.46	2.28	2.49	2.95

Final Deformation Indicator for Lock Head. By summing water pressure, temperature, and time-dependent components, secondary deformation indicators for the lock head measurement points are established for each season (Table 6). Recorded measurements for all conditions were below these indicators, confirming structural stability.

Table 6. Secondary Deformation Monitoring Indicators for Measurement Points (mm)

Condition	Measurement Point	Measurement Point Elevation (m)	Secondary Monitoring Indicator				Measured Maximum Value	Difference with Max
			Dec.-Feb.	Mar.-May	Jun.-Aug.	Sept.-Nov.		
Normal Operation	PL03CZ331	156.5	6.47	6.64	7.30	7.06	3.06	4.24
	PL05CZ321	156.5	7.85	7.72	8.54	8.75	4.63	4.12
Low Water Condition	PL03CZ331	156.5	6.93	7.10	7.76	7.52	3.06	4.40
	PL05CZ321	156.5	8.53	8.4	9.22	9.43	4.63	4.80

4 Conclusion

This study proposes secondary deformation monitoring indicators for a reinforced lock head based on a hybrid model that integrates numerical and statistical deformation analysis. Key findings include:

Deformation in the side slopes is mainly influenced by unloading of the surrounding rock, while deformation in the lock head is affected by water level, temperature, and time-dependent factors, with minimal impact from gate opening. Deformation in the lock head is sensitive to degradation of material properties, which should be closely monitored as a primary control factor. Due to significant annual temperature variations in the project area, monthly-based deformation monitoring indicators can more accurately reflect the operational state of the structure, which is beneficial for ensuring project safety.

The hybrid model demonstrates strong interpretability, lower complexity, and reliable accuracy in establishing secondary deformation monitoring indicators for reinforced lock heads, making it well-suited for engineering applications and broader adoption.

Although current results indicate stable performance of the project, However, due to the influence of operating conditions, on-site personnel should regularly use the proposed method to verify monitoring indicators, ensuring structural safety and reliability.

Acknowledgements

the National Key R&D Program of China (2023YFC3206103), the National Natural Science Foundation of China (52309152, U23B20150), the Natural Science Foundation of Jiangsu Province (BK20220978), and the Open Fund of National Dam Safety Research Center (Grant No. CX2023B03).

References

1. Ranković V, Grujović N, Divac D, Miliivojević N. Development of support vector regression identification model for prediction of dam structural behaviour[J]. *Structural Safety*. 2014, 48:33-39. <https://doi.org/10.1016/j.strusafe.2014.02.004>.
2. Zhu Y, Niu X. Residual correction-based dam deformation monitoring method via data dimension reduction and optimized Bi-LSTM algorithm[J]. *Structural Health Monitoring*, 2024. Early Access. <https://doi.org/10.1177/14759217241264098>.
3. Wu Z. Safety diagnosis and hidden defects detection of major hydraulic concrete structures [M]. Beijing: Higher Education Press, 2006. <https://xuanshu.hep.com.cn/front/book/find-BookDetails?bookId=59cc7441ba9eb884cf8170b8>.
4. Cong P, Gu C, Gu Y. Maximum Entropy Method for Determining Dam Safety Monitoring Indices[J]. *Geomatics and Information Science of Wuhan University*, 2008, 33(11): 1126-1129. <https://doi.org/10.13203/j.whugis2008.11.013>.
5. Li Z, Hou H. Dam safety monitoring indices based on motion stability theory[J]. *Engineering Journal of Wuhan University*, 2010,43(05):581-584+607. <http://ch.whu.edu.cn/cn/article/pdf/preview/1764.pdf>.
6. Jia D, Ma C, Yang J, et al. Method for determining displacement monitoring indexes of arch dams based on stochastic back analysis of parameters [J]. *Journal of Hydroelectric Engineering*, 2024, 43(1): 124-133. <https://doi.org/10.11660/slfdx.20240111>.
7. Zhu Y, Xie M, Zhang K, et al. A Dam Deformation Residual Correction Method for High Arch Dams Using Phase Space Reconstruction and an Optimized Long Short-Term Memory Network. *Mathematics*, 2023,11, 2010. <https://doi.org/10.3390/math11092010>.
8. Wang H, Niu X, Xu L, et al. Dam deformation prediction model based on singular spectrum analysis and improved whale optimization algorithm-optimized BP neural network[J]. *Journal of Hydroelectric Engineering*, 2023, 42(11): 136-145. <https://doi.org/10.11660/slfdx.20231113>.
9. Zhu Y, Zhang Z, Gu C, et al. A Coupled Model for Dam Foundation Seepage Behavior Monitoring and Forecasting Based on Variational Mode Decomposition and Improved Temporal Convolutional Network[J]. *Structural Control and Health Monitoring*, 2023: 3879096. <https://doi.org/10.1155/2023/3879096>.

Open Access This chapter is licensed under the terms of the Creative Commons Attribution-NonCommercial 4.0 International License (<http://creativecommons.org/licenses/by-nc/4.0/>), which permits any noncommercial use, sharing, adaptation, distribution and reproduction in any medium or format, as long as you give appropriate credit to the original author(s) and the source, provide a link to the Creative Commons license and indicate if changes were made.

The images or other third party material in this chapter are included in the chapter's Creative Commons license, unless indicated otherwise in a credit line to the material. If material is not included in the chapter's Creative Commons license and your intended use is not permitted by statutory regulation or exceeds the permitted use, you will need to obtain permission directly from the copyright holder.

